Dinuclear Paramagnetic Metallocenes Bridged by Silyl Groups – Synthesis and Intramolecular Interactions

Hermann Atzkern[a], Pierre Bergerat[b], Monika Fritz[a], Johann Hiermeier[a], Peter Hudeczek[a], Olivier Kahn[b], Basil Kanellakopulos[c], Frank H. Köhler*[a], and Michael Ruhs[a]

Anorganisch-chemisches Institut der Technischen Universität München[a],
Lichtenbergstraße 4, D-85747 Garching

Université de Paris-Sud, Laboratoire de Chimie Inorganique[b],
CNRS URA 420, F-91405 Orsay

Institut für Heisse Chemie, Kernforschungszentrum Karlsruhe[c],
Postfach 3640, D-76344 Eggenstein-Leopoldshafen

Received July 14, 1993

Key Words: Metallocenes, dinuclear, silyl-bridged / Antiferromagnetism / Cyclic voltammetry / Paramagnetic NMR spectroscopy

The dilithium salt of the 3a,4,7a,8-tetrahydro-4,4,8,8-tetramethyl-4,8-disila-*s*-indacenediyl dianion (L^{2-}, **2**) was allowed to react with the solvated metal halides MX_2 (M = Ni, Co, Cr) in the presence of the cyclopentadienyl (Cp) anion to give *trans*-CpMLMCp (**3NiNi**, **3CoCo**, and **3CrCr**) in yields up to 80%. The only *cis* isomers which could be detected were **4NiNi** and **4CoCo**. Similarly, the reaction of **2** with $[CpVCl(PEt_3)]_2$ gave the *trans*-vanadium analogue **3VV** while the successive reaction of **2** with $CrCl_3(THF)_3$ and PEt_3 yielded the bridged half-sandwich $(Et_3P)Cl_2CrLCrCl_2(PEt_3)$ (**5CrCr**). The mixed-metal dinuclear metallocene CpFeL-NiCp (**3FeNi**) was synthesized from $CpFeL^-$, Cp^- and solvated $NiBr_2$. The molecules were characterized by mass spectrometry, elemental analyses, cyclic voltammetry, ^{1}H-, ^{13}C-, and ^{29}Si-NMR spectroscopy and solid-state magnetic measurements. Cyclic voltammetry showed up to six electron transfers per molecule. A metal-dependent splitting of the half-wave potentials of up to 355 mV indicated rather strong electrostatic interaction between the metallocene units. The NMR results established unpaired spin on the ligands. Its distribution within the bridging ligand was correlated with the molecular orbital splitting and the magnetic interaction. Antiferromagnetic interaction was found for **3NiNi**, **3CrCr**, and **3VV** with $J = -11.6$, -2.56, and -1.34 cm^{-1}, respectively ($H = -J \cdot \mathbf{S}_A \cdot \mathbf{S}_B$). A temperature-dependent folding of the bridging ligand was deduced from the temperature behavior of the ^{1}H-NMR signal shifts.

The paramagnetic metallocenes Cp_2M (Cp = cyclopentadienyl) are promising building blocks for polynuclear magnetic materials because various spin states are available. For the neutral species these are S = 1/2 (Cp_2Co and low-spin Cp_2Mn), S = 1 (Cp_2Cr, Cp_2Ni), S = 3/2 (Cp_2V), and S = 5/2 (high-spin Cp_2Mn). When the metallocenes are tied together by starting from bridged Cp anions of type **1**, polymeric materials are expected which may have properties different from those of Cp_2M. There is a long-standing interest in such properties[1], but they may be difficult to probe when the materials are not well-defined or when they cannot be purified sufficiently. An obvious way out of this dilemma is the study of suitable model compounds. For instance, this has been demonstrated for electrostatic interactions[2], and one of us[3] has outlinted the power of the approach when the magnetic properties of coordination compounds are concerned.

As a specific example of **1** we have synthesized the dianion **2** where two Me_2Si groups serve as short bridges which limit the relative orientation of the two Cp units[4].

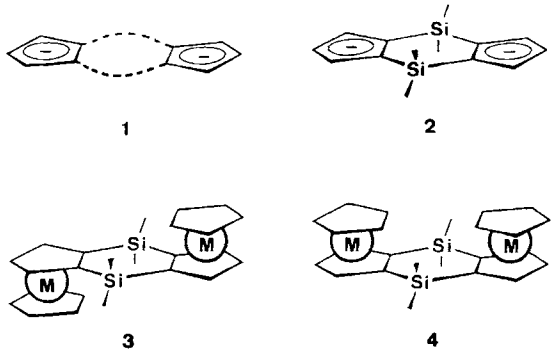

1 **2** **3** **4**

Ligand **1** and its alkyl derivatives have also been used by Jutzi and Siemeling[5a–c] and by Brintzinger[5d] while Nifant'ev and Ustynyuk have synthesized analogues with metal and carbon bridges[6]. The most simple model compound derived from **2**, which is susceptible to intramolecular interactions between metallocenes, is the dinuclear species. It may exist as the *trans* and *cis* isomer **3** and **4**,

  0009–2940/94/0202–0277 $ 10.00+.25/0

respectively. In this paper we report on dinuclear vanadocenes, chromocenes, cobaltocenes, and nickelocenes as well as on an FeNi derivative and a dinuclear chromium(III) half-sandwich. Preliminary results on the bridged chromocenes have been published[7].

Results

Syntheses

Most of the homodinuclear bridged metallocenes were synthesized by treating a mixture of the dianion **2** and CpNa in THF with the corresponding metal dihalides solvated by THF or NEt_3 (Scheme 1). A tenfold excess of CpNa was used in order to limit the formation of products containing more than two bridged metallocenes. An excess of Cp_2M, which was present in the crude product, could be accepted because it was easily removed by sublimation. In the case of nickel it could be demonstrated that the procedure is rather efficient (80% yield of **3NiNi**).

Scheme 1

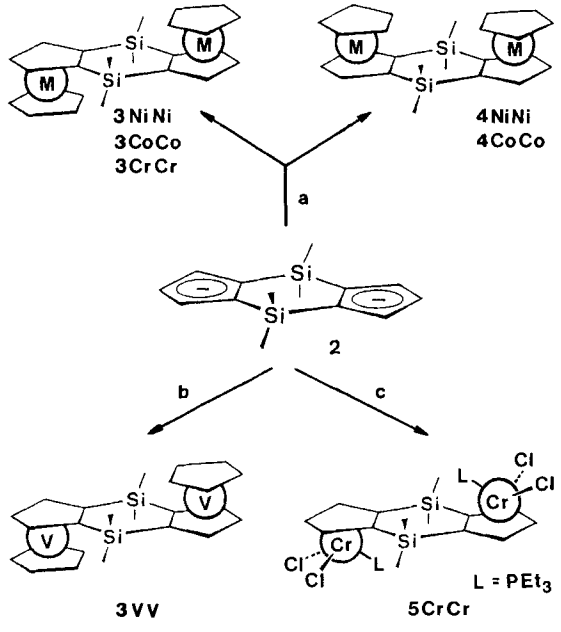

a: Cp^-, MX_2. – b: $[CpVCl(PEt_3)]_2$. – c: $CrCl_3(THF)_3$, PEt_3.

Medium-pressure liquid chromatography (MPLC) of the nickelocenes, which remained after sublimation, showed that a trace of Cp_2Ni was still present and that only 2% of a trinuclear species could be extracted with hexane. The main fraction contained the dinuclear nickelocenes. After crystallization, the ^{1}H-NMR investigation of the mother liquor revealed that besides the *trans* product (**3NiNi**) little *cis* isomer (**4NiNi**) was also present. In a second MPLC run it was possible to enrich **4NiNi** to about 90% as indicated by the ^{1}H-NMR spectrum represented in Figure 1. All pairs of isomers **3MM/4MM** may be distinguished easily by the number of their CH_3 proton signals.

For cobalt a similar procedure gave a crude product, which after sublimation of Cp_2Co contained 68% of **3CoCo**, 20% of **4CoCo**, 6% of the *trans,trans* trinuclear

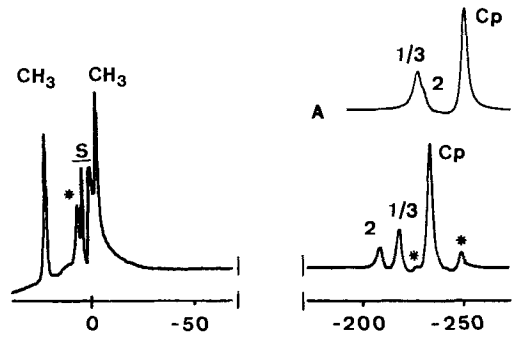

Figure 1. ^{1}H-NMR spectrum of **4NiNi** containing some **3NiNi** (starred signals); signals above $\delta = 200$ with double intensity; insert A shows the corresponding signal pattern of pure **3NiNi**; temperature 305 K, S = solvent ($[D_8]$toluene)

species (not isolated), 5% of Cp_2Co, and traces of higher nuclear cobaltocenes. Attempts to separate the *cis/trans* isomers **4CoCo** and **3CoCo** by chromatography failed. By contrast, fractional crystallization gave analytically pure **3CoCo** although the ^{1}H-NMR spectrum disclosed a trace of Cp_2Co. **4CoCo** could be enriched by crystallization to yield a 3:2 mixture of **4CoCo/3CoCo**. The dinuclear chromocene **3CrCr** could be purified similarly. Rapid crystallization was necessary in order to limit the formation of a grey-brown powder which accompanied the red-brown crystals of **3CrCr**. The vanadium compound **3VV** (Scheme 1) was synthesized via the half-sandwich $[CpVCl(PEt_3)]_2$[8] which was not isolated. The yield of **3VV** after crystallization (26%) suffered from the formation of some slurry together with the desired dark violet crystalline compound.

When the dianion **2** was treated successively with $CrCl_3(THF)_3$ and PEt_3 the homodinuclear half-sandwich **5CrCr** was obtained in 82% yield. The dark blue compound resembles the mononuclear donor adducts of $CpCrX_2L$ which we and others[9] have synthesized previously.

A different approach had to be used for the synthesis of the heterodinuclear metallocene **3FeNi** (Scheme 2). It was based on the stepwise formation of **2** which allowed us to synthesize the anion **6**[10]. Its reaction with THF-solvated $NiBr_2$ in the presence of an excess of CpNa gave a mixture of nickelocenes from which Cp_2Ni was removed by sublimation. MPLC afforded pure **3FeNi** in 71% yield.

Scheme 2

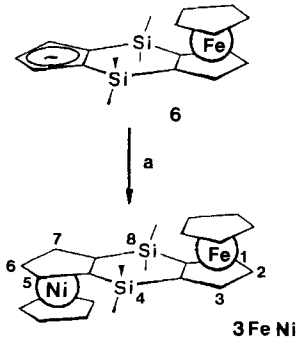

a: Cp^-, $NiBr_2(THF)_{1.5}$.

Table 1. Electrochemical data[a] of the dinuclear metallocenes **3CrCr**, **3FeFe**[b], **3CoCo**, and **3NiNi** compared to those of the parent metallocenes

	3CrCr	**3FeFe**[b]	**3CoCo**	**3NiNi**	Cp_2Cr	Cp_2Fe	Cp_2Co	Cp_2Ni
$E_{1/2}(1)$	240	1280	0	895	240	1345[f]	0	905
$\Delta E_p(1)$	55	80	60	65	65	75[g]	65	100[h]
$E_{1/2}(2)$	455	1490	165	1045	–	–	–	1850
$\Delta E_p(2)$	55	80	60	65	–	–	–	115[h]
$\Delta E_{1/2}(2/1)$	215	210	165	150	–	–	–	–
$E_{1/2}(3)$	–	–	–	1885	–	–	–	–
$\Delta E_p(3)$	–	–	–	85	–	–	–	–
$E_{1/2}(4)$	–	–	–	2015	–	–	–	–
$\Delta E_p(4)$	–	–	–	[c]	–	–	–	–
$\Delta E_{1/2}(4/3)$	–	–	–	130	–	–	–	–
$E_{1/2}(-1)$	−1215	–	−910	−1095[d]	−1310	–	−960	[h,i]
$\Delta E_p(-1)$	70	–	65	–	95	–	85	–
$E_{1/2}(-2)$	−1540	–	−1110	−1450[d]	–	–	–	–
$\Delta E_p(-2)$	115	–	65	–	–	–	–	–
$\Delta E_{1/2}(-1/-2)$	325	–	200	355[e]	–	–	–	–

[a] In mV relative to Cp_2Co/Cp_2Co^+ at −20°C except for **3FeFe** and Cp_2Ni; concentration $0.7-1.3 \cdot 10^{-3}$ mol l^{-1} (**3MM**) and 1.3–3.2 mol l^{-1} (Cp_2M) in propionitrile, supporting electrolyte 0.1 M n-Bu_4NPF_6, scan rate 200 mVs^{-1}. – [b] From ref.[11]. – [c] Reverse peak not well resolved. – [d] Cathodic waves $E_c(-1)$ and $E_c(-2)$. – [e] $\Delta E_c(-1/-2)$. – [f] 1325 mV at 25°C. – [g] 85 mV at 25°C. – [h] Cell not optimized. – [i] Not observed.

The new compounds in Schemes 1 and 2 are air-sensitive; special care is necessary for the dinuclear cobaltocenes, vanadocenes, and chromocenes, the latter being pyrophoric. The solubility increases on passing from acetonitrile and hexane to toluene and THF.

Cyclic Voltammetry

The cyclic voltammograms (CVs) have been measured for solutions of **3CrCr**, **3CoCo**, and **3NiNi** in propionitrile which is well suited for the separation of successive electron transfers (ETs)[11]. In Table 1 the data that we obtained are compared with those of **3FeFe**[11]. The parent metallocenes have also been investigated because it is known that the half-wave potentials ($E_{1/2}$) vary with the solvent, and no data for solutions in propionitrile is available in the literature. The $E_{1/2}$ values were determined by using internal reference compounds in order to compensate the drift of the potential of the reference electrode[12]. The chromocenes and ferrocenes were measured relative to Cp_2Co/Cp_2Co^+ while the cobaltocenes and nickelocenes were measured relative to Cp_2Fe/Cp_2Fe^+ and calculated relative to Cp_2Co/Cp_2Co^+.

The CV of **3NiNi** comprises six ETs four of which are oxidations leading to the tetracation, while the remaining two ETs yield the dianion. As judged from the separation of the anodic and cathodic peak potentials (ΔE_p) given in Table 1 most of the ETs of the dimetallic derivatives show a better reversibility than those of the parent metallocenes. Typical CVs are reproduced in Figure 2. Within the error limits the ETs of **3CoCo** and the first two ETs of **3CrCr** and **3NiNi** are electrochemically reversible, whereas the other ETs are quasi-reversible. An exception is the fourth oxidation of **3NiNi**. The poor reverse peak indicates that part of the tetracation reacts before it is reduced back to the trication. Further experiments are necessary to show whether intermolecular reactions are responsible, which have been described for similar molecules[11,13]. Both reductive ETs of **3NiNi** are irreversible at −20°C. This is in accord with earlier reports which claim a reversible reduction of Cp_2Ni only below −60°C[14].

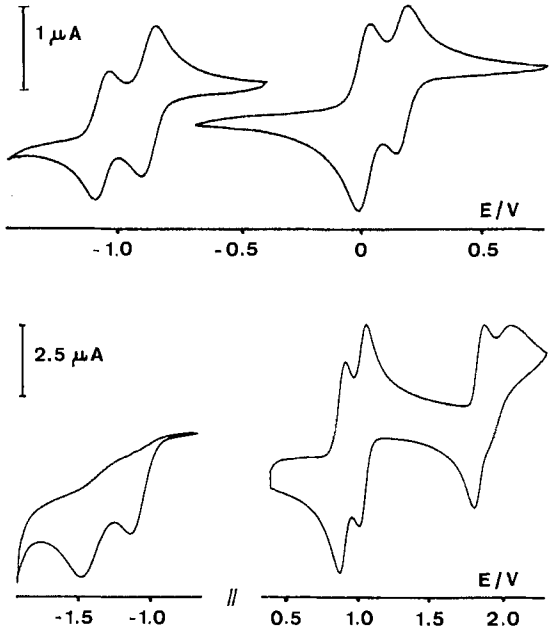

Figure 2. Cyclic voltammograms of **3CoCo** (top) and **3NiNi** (bottom) in propionitrile; concentration $0.9 \cdot 10^{-3}$ (top) and $1.3 \cdot 10^{-3}$ (bottom), 0.1 mol l^{-1} n-Bu_4NPF_6, 200 mVs^{-1}, potential vs. Cp_2Co/Cp_2Co^+

Two oxidative and two reductive ETs were observed for **3CoCo** as expected for a dinuclear cobaltocene. It is worth noting that **3CoCo**$^-$ and **3CoCo**$^{2-}$ showed no instability at −20°C in propionitrile and a scan rate of 50 mVs^{-1} whereas Geiger[15] has reported an ECE mechanism for the reduction of Cp_2Co in acetonitrile.

Similar improvements were found for the CV of **3CrCr** which has been described briefly[7]. Thus, all ETs were

Table 2. Paramagnetic ^{1}H-, ^{13}C-, and ^{29}Si-NMR signal shifts[a] of the dinuclear metallocenes **3MM**, **4MM**, and **3FeNi** at 298 K

Nuclei[b]	**3NiNi**[c]	**4NiNi**[c]	**3CoCo**[c]	**4CoCo**[c]	**3CrCr**[c]	**3VV**[c]	**5CrCr**[d]	**3FeNi**[e] nuclei near Fe	**3FeNi**[e] nuclei near Ni
Cp-H	263	−246	−55.8	−53.6	314	316	–	−3.1	−259
1,3,5,7-H	−241	−221	−35.8	−20.3	256	262	252	0.5	−236
2,6-H	−243	−231	−60.2	74.3	208	262	252	2.2	−241
CH_3	10.9	26.9[f] −4.2	4.0	8.9[f] −0.3	−5.5	28.6	5.5	−2.5[g]	6.0[g]
Cp-C	1430	–	531	516	−300	−575	51.9	39.0	[h]
C-3a,8a,4a,7a	1430	–	545	606	−297	−536	36.8	136.0	[h]
C-1,3,5,7	1430	–	414	222	−554	−484	152.9	5.1	[h]
C-2,6	1505	–	733	893	−78.5	−561	27.1	38.8	[h]
CH_3 (C-β)	479	–	145	341[f] 52	−63.6	−75.4	–	101.2[g]	242[g]
Si-4,8 (Si-α)	−1765[i]	–	−432	−447	–	–	–	–	−848[j]

[a] Shifts relative to an isostructural diamagnetic compound (cf. Experimental). – [b] The numbering is given in Scheme 2. – [c] In [D_8]toluene. – [d] ^{1}H NMR in $CDCl_3$, ^{13}C NMR in CH_2Cl_2; signal shifts of coordinated $P(Et)_3$: δ = 43.8 (α-H), −5.5 (β-H); 288.3 (C-α), −36.6 (C-β). – [e] ^{1}H NMR in [D_6]acetone, ^{13}C NMR in THF. – [f] CH_3 group pointing to the metal (cf. Figure 6C and discussion). – [g] Assignment tentatively; the larger shift corresponds to the nuclei pointing to Ni. – [h] Signal-to-noise ratio insufficient. – [i] At 337 K. – [j] At 328 K.

found to be reversible except for the process **3CrCr**$^-$ → **3CrCr**$^{2-}$ which is quasi-reversible. Under similar conditions, Cp_2Cr^- is unstable in acetonitrile[14a].

^{1}H-, ^{13}C- and ^{29}Si-NMR Spectroscopy

All new compounds have been characterized by their ^{1}H- and ^{13}C-NMR spectra, and selected compounds have also been studied by ^{29}Si-NMR spectroscopy; the results are collected in Table 2. As expected for paramagnetic metallocenes the signal shifts (δ^{para}) are large. They cover ranges larger than δ = 500 and 2000 for ^{1}H and ^{13}C, respectively. The signal assignment follows from the typical ranges where the signals of other metallocenes, in particular silylated derivatives[16a], have been found. For the *cis* isomers **4NiNi** and **4CoCo** as well as for **3FeNi** the assignment of the methyl signals is based on the distortion of the molecules discussed below. Remarkably, the ^{1}H- and ^{13}C-NMR relaxation time in position 1,3 of **4CoCo** is long enough to allow the observation of a doublet in the ^{13}C-NMR spectrum. All other doublets in the series of compounds remained unresolved.

The NMR signals show a temperature dependence which can best be measured for the ^{1}H nuclei and which deviate from the Curie law. This is demonstrated in Figure 3a and b where the reduced shifts [$\vartheta(^1H) = \delta^{para}(^1H)T/298$] are plotted versus T; $\vartheta(^1H)$ is comparable to the molar magnetic susceptibility (χ_m) multiplied by T (cf. below) which is expected to give parallels to the T axis when pure paramagnetism with only one thermally populated state is present.

Magnetism

Solid-state magnetic measurements have been carried out for **3NiNi**, **3CrCr**, and **3VV** down to 1.3 K. A double check down to 77 K with a second sample of **3CrCr** confirmed the results. The magnetic behavior of the dinuclear metallocenes is reflected in the $\chi_m T$-versus-T plots given in Figure 4.

In Table 3 the high-temperature $\chi_m T$ values are compared to what is expected when the magnetic interaction parameter J is zero. In all cases the agreement is very good. When the temperature is lowered $\chi_m T$ decreases as illustrated in Figure 4 and reaches values at 1.3 K which are smaller by a factor of 9 to 30. This behavior can be accounted for by antiferromagnetic interaction and the local anisotropy.

For each compound the theoretical molar magnetic susceptibility χ_m was calculated as follows: The susceptibility along the u axis $\chi_{m,u}$ is defined as

$$\chi_{m,u} = \frac{N\beta}{H_u} \frac{\Sigma_i(-\partial E_{i,u}/\partial H_u)\exp(-E_{i,u}/kT)}{\Sigma_i \exp(-E_{i,u}/kT)} \quad (1)$$

where the energies $E_{i,u}$ are the eigenvalues of the spin Hamiltonian

$$H_u = -J\mathbf{S_A}\cdot\mathbf{S_B} + \mathbf{S_A}\cdot\mathbf{D}\cdot\mathbf{S_A} + \mathbf{S_B}\cdot\mathbf{D}\cdot\mathbf{S_B} + \beta g_u(\mathbf{S_A}+\mathbf{S_B})\cdot H_u \quad (2)$$

J is the isotropic interaction parameter, $\mathbf{S_A}$ and $\mathbf{S_B}$ are the local spin operators, $\mathbf{D}$ is the local anisotropy tensor, g_u the Zeeman factor along the u direction, and H_u the applied magnetic field along the same direction. In eq. (2), the anisotropic interaction is assumed to be negligibly small with respect to the local anisotropy. The average magnetic susceptibility is calculated through

$$\chi_m = (4\pi)^{-1} \int_{space} \chi_m(\theta,\phi)\sin\theta d\theta d\phi \quad (3)$$

Furthermore, it was assumed that the local anisotropy was axial, the axial zero-field splitting parameter D being related to the elements D_{uu} of the $\mathbf{D}$ tensor through

$$D = 3D_{zz}/2 \quad (4)$$

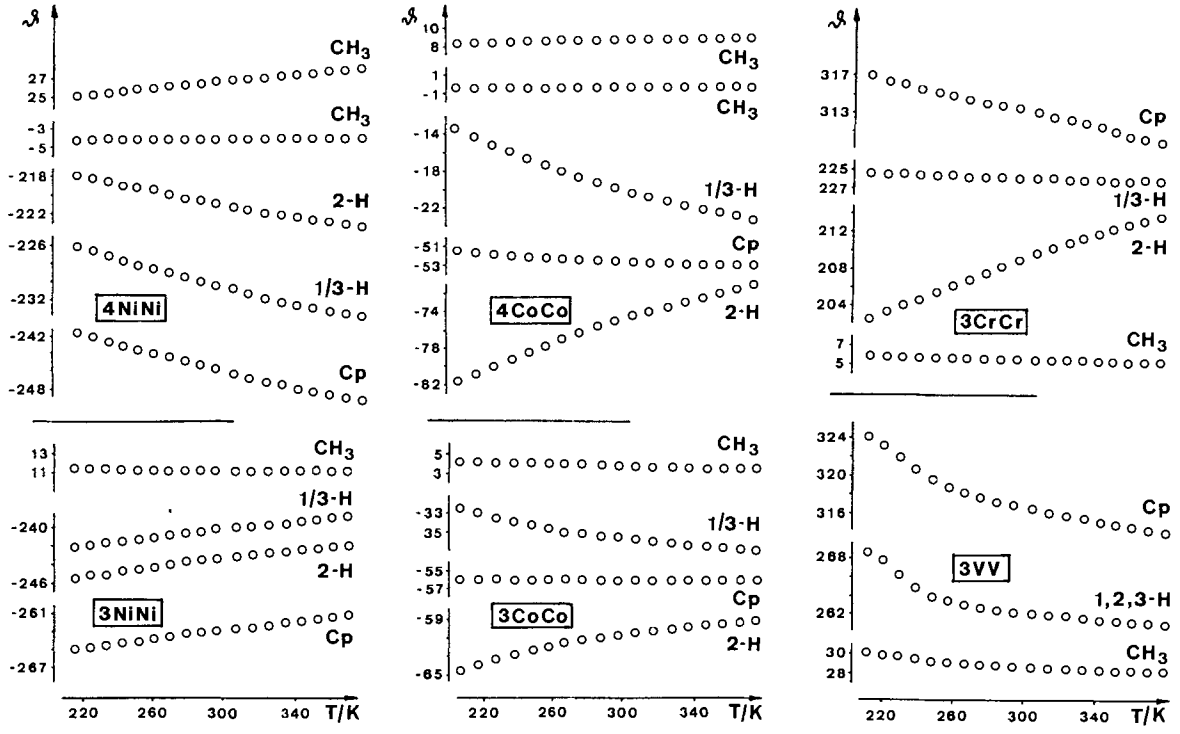

Figure 3a. Temperature-dependent ^{1}H-NMR results of **3NiNi**, **4NiNi**, **3CoCo**, **4CoCo**, **3CrCr**, and **3VV** given as reduced shifts ϑ vs. T (cf. text)

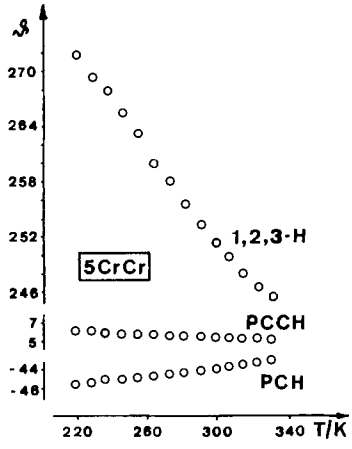

Figure 3b. ^{1}H-NMR results as in Figure 3a for **5CrCr**

For the fitting of the experimental data of **3NiNi** and **3VV**, we used the D and g parameter values deduced from the magnetic and/or EPR properties of nickelocene[18] and vanadocene[19], respectively. For **3CrCr** we used D and g values obtained by reinterpreting the magnetic properties of chromocene[20] with a spin Hamiltonian of the form

$$H = \mathbf{S}_{Cr} \cdot \mathbf{D} \cdot \mathbf{S}_{Cr} + \beta \mathbf{S}_{Cr} \cdot \mathbf{g} \cdot \mathbf{H} \qquad (5)$$

When an average g value was used, the high temperature limit of $\chi_m T$ could not be reached (Figure 4). The result was improved by using an axial **g** tensor (fit II in Table 3) as can be seen from the agreement factor R defined as

$$R = \Sigma[(\chi_m T)^{obs} - (\chi_m T)^{cal}]^2 / \Sigma[(\chi_m T)^{obs}]^2 \qquad (6)$$

A deviation from the experimental data between 20 and 150 K remains unexplained, but it is clear that J, the parameter of interest, hardly changes.

Discussion

Formation of *cis*/*trans* Isomers

The reactions illustrated in Scheme 1 should lead to both *cis* and *trans* isomers. Under the conditions described in the experimental part we were able to isolate the *trans* isomers in all cases. By contrast, the *cis* isomers could only be established for nickel and cobalt (**4NiNi** and **4CoCo**) although, for the other metals, they should be easy to detect by ^{1}H-NMR spectroscopy especially when looking at the CH_3 signals. In the case of nickel the *trans* isomer predominates, and a trace of the *cis* isomer could be detected only after enrichment by MPLC and crystallization.

For the FeNi mixed-metal compound we have investigated this in more detail because both the MPLC separation and the analysis by ^{1}H-NMR spectroscopy are most efficient. The latter is due to the fact that rather narrow signals of the ferrocene moiety are available. No *cis* isomer was observed when the reaction was run in boiling ether (35°C). When the temperature was increased to boiling THF (66°C) or di-*n*-butyl ether (141°C) nothing changed except that the yield of **3FeNi** dropped somewhat from 71 to 64 and 68%, respectively.

We have discussed steric requirements and the type of the metal–Cp bond on the formation of *cis*/*trans* isomers

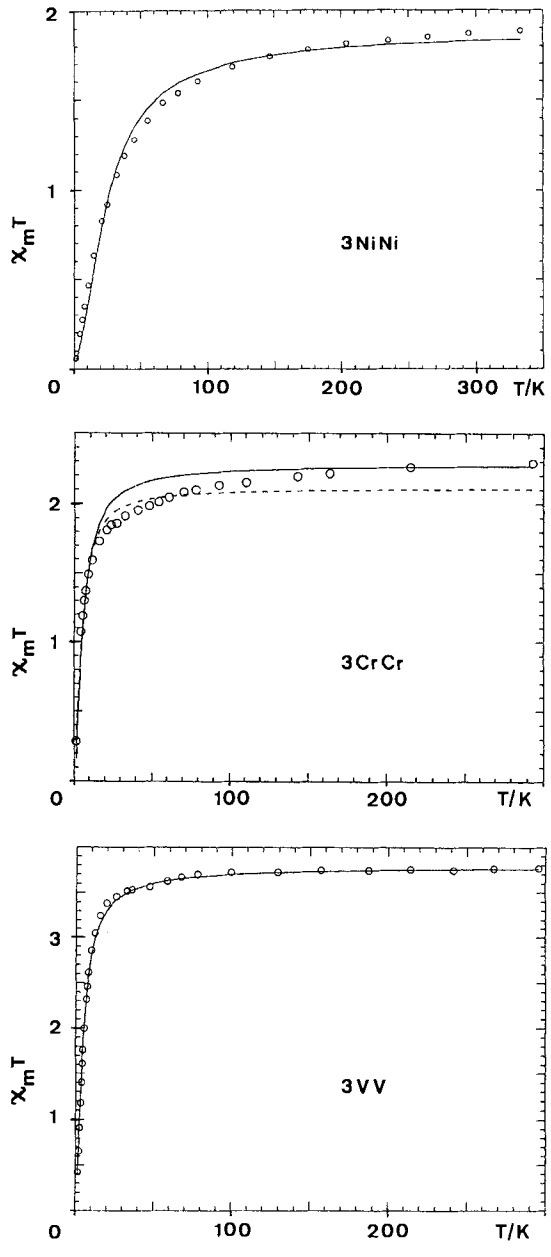

Figure 4. $\chi_m T$-versus-T plots of **3NiNi**, **3CrCr**, and **3VV**; the parameters of the best-fit curves are given in Table 3; the broken curve corresponds to fit I; $\chi_m T$ in cm^3 K mol^{-1}

Table 3. Magnetic data[a] of the dinuclear metallocenes **3NiNi**, **3CrCr**, and **3VV**

	3NiNi	3CrCr fit I	3CrCr fit II	3VV
$\chi_m T$ (J = 0)[b]	1.90		2.29	3.78
$\chi_m T$ (298 K)	1.87		2.28	3.78
$\chi_m T$ (1.3 K)	0.0615		0.228	0.422
g[c]	1.95	2.07	1.89[d] 2.25[e]	2.01
D[c]	27.5	11	11	2.5
J	−11.6	−2.56	−2.25	−1.34
R · 10^3	1.8	16	3.8	0.16

[a] $\chi_m T$ in cm^3 K mol^{-1}, D and J in cm^{-1}. – [b] $\chi_m T$ expected for the magnetically uncoupled species. – [c] Fixed values (see text). – [d] $g_{\|}$. – [e] $g_{\perp}$.

earlier[11] while comparing the dinuclear ferrocenes and the dilithium salt of **2**. There is no obvious extension of these ideas to other transition metals at present.

Electrostatic Interactions

When we pass from the parent metallocenes to the dinuclear congeners in Table 1 all ETs undergo a splitting given as $\Delta E_{1/2}$. This is indicative of an interaction within the bridged metallocenes which we have shown previously[11] to be mainly due to the effect of an adjacent charge on the ET.

Two trends are observed for $E_{1/2}$. One is the change with the formal oxidation state of the metal. When we take **3NiNi** as an example and when we proceed from Ni^{I} to Ni^{II} and Ni^{III} the splitting and thus the interaction decreases from 355 to 150 and 130 mV. The first value is actually the difference between the two cathodic peak potentials, but the same trend is found for the reversible ETs of **3CoCo** and **3CrCr**. For an explanation we can think of differences in the solvation of the species, depending on the external charge, or a change in the folding of the bridging ligand which influences the metal-metal distance (cf. below).

The second trend is the increase of the corresponding $\Delta E_{1/2}$ values on going from **3CoCo** to **3FeFe**, **3CrCr**, and **3NiNi**. It is reasonable to assume that, for a given external charge, the solvation does not change very much with the metal. By contrast, a metal-dependent folding of the molecules is likely to occur because of the differences in the Cp–metal distances[17] (cf. Figure 6 and the discussion below). Therefore we conclude that both trends are influenced by geometrical changes.

Distribution of the Unpaired Electrons

From the NMR data of the new compounds given in Table 2 and the fact that the dipolar signal shifts are small[21] ist is clear that a considerable part of the unpaired spin is delocalized onto the ligand. The signs of the signal shifts and thus the signs of magnetic moment associated with the spin density are in perfect agreement with a direct π delocalization onto the ligand for the nickel and cobalt derivatives while π polarization and direct σ delocalization operate within the chromium and vanadium derivatives[16].

The spin distribution within the ligand of the dinuclear cobaltocenes **3CoCo** and **4CoCo** should follow the splitting of the orbitals, their population, and their ligand π orbital content as illustrated in Figure 5. The splitting arises from the lowering of the symmetry of Cp by two Me_2Si bridges in a similar way as for $(Me_3SiCp)_2Co$[16a]. However, the energy gap ΔE^2 between π_a and π_s, and hence the difference of the population by unpaired spin, should be smaller than for ΔE^1. Since the NMR signal shifts reflect the squared carbon $2p_z$ coefficients (cf. Figure 5) this should be visible in the spectra. In fact, the ^{13}C-NMR signal sequence of **3CoCo** (Table 2) is the same as that of $(Me_3SiCp)_2Co$, and the splitting of these signals is smaller for **3CoCo**. Surprisingly, the splitting of the ^{13}C-NMR signals of C-1,2,3,3a,8a is much larger for the *cis* isomer **4CoCo** than for the *trans* isomer **3CoCo**. From this we conclude that in addition to

the substituent-derived splitting of π_a and π_s there is also a contribution from lowering the molecular symmetry by a folding of the bridging ligand which changes the spin delocalization from the metal to the ligand. This effect must be more pronounced for **4CoCo** than for **3CoCo**; it has been considered above in order to explain the result obtained from cyclic voltammetry.

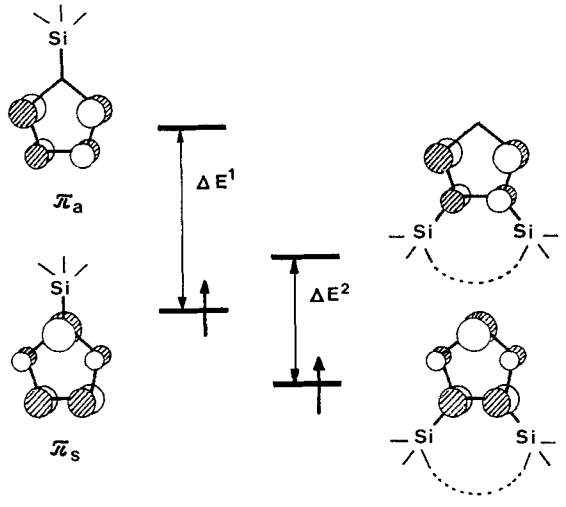

Figure 5. Ligand orbitals contributing to the spin-containing e_1-type orbitals of silylated cobaltocenes and their qualitative energy splitting; the radii of the atomic orbitals qualitatively follow the coefficients of the carbon $2p_z$ orbitals; the unpaired electrons partly occupy the upper level

For the nickelocenes **3NiNi** and **4NiNi** the signal splitting for the nuclei of the five-membered ring atoms is small as expected[16,22], but it is visible in the ^{1}H-NMR spectra. Note that, as for the cobaltocenes, the signal splitting is larger for the *cis* isomer **4NiNi** than for **3NiNi**. In addition, the signal sequence of 2-H and 1,3-H is inverted on going from **3NiNi** to **4NiNi**. In the light of our earlier discussion[22] this is another indication of a geometric contribution to the splitting of π_a and π_s.

The chromium derivatives **3CrCr** and **5CrCr** as well as **3VV** are less clear-cut examples because the spin distribution is influenced not only by π polarization but also by σ delocalization. A striking example is **3CrCr** for which the signal sequence of the five-membered ring atoms depends on whether ^{1}H or ^{13}C is investigated.

In terms of magnetic interaction the spin on the bridging nuclei is of special interest. When two paramagnetic metallocenes are connected by Me_2Si the spin densities at the nuclei in the α position (α relative to Cp) simply add. This follows from the ^{29}Si-NMR signal shift for **3NiNi** (δ = −1765) which is approximately twice as large as that for **3FeNi** (δ = −848) and for $(Me_3SiCp)_2Ni$ (δ = −904[23]). Interestingly, the $\delta^{para}(^{29}Si)$ value of **3CoCo** (δ = −432) is by far less than twice that of $(Me_3SiCp)_2Co$ (δ = −355[22]). The reason for this is evident from Figure 5: For **3CoCo** the level associated with π_a is more populated than for $(Me_3SiCp)_2Co$ so that the spin density at C-3a,4a,7a,8a of **3CoCo** is smaller.

The spin density at the nuclei in the β position is determined by two factors: the additive contribution of two metallocenes and selective spin transfer owing to hyperconjugation. The hyperconjugative increase of spin density shows up when **3NiNi** is compared with $(Me_3SiCp)_2Ni$ which has δ^{para}(C-β) = 209[16a]. Hence, for **3NiNi** we expect a signal shift of little more than δ = 400 which must be compared with the experimental shift of δ = 479 (Table 2). The increase of the shift and thus the spin density is related to the change of the dihedral angle between the bond Si−C-β and the spin-carrying $2p_z$ orbital of C-3a,4a,7a,8a; it is more favorable for **3NiNi** (ca. 30°) than for $(Me_3SiCp)_2Ni$ (45°). This reasoning has been treated in more detail earlier[16b]. It should be noted that a quantitative comparison of **3MM** and $(Me_3SiCp)_2M$ is somewhat misleading because there are also changes in the metal−Cp bond and, for M = Co and Cr, in the MO population similar to that shown in Figure 5. However, we may conclude qualitatively from the $\delta^{para}(^{13}C$-$\beta)$ values in Table 2 that the spin density in the bridge of **3MM** has been increased for M = Ni whereas it is rather small for M = Cr and V.

Magnetic Interactions

The deviation of the temperature-dependent NMR signal shifts of di- and oligonuclear compounds from the Curie law may indicate magnetic interactions, and this has been demonstrated for a number of Cp metal compounds[9a,24]. However, the deviation may also be due to a temperature-dependent change of the population of near-degenerate orbitals which accommodate one unpaired electron (cf. Figure 5). Substituted mononuclear cobaltocenes and chromocenes are typical examples[23,25]. The ϑ-T plots of **3CoCo**, **4CoCo**, and **3CrCr** can be explained in this way, and they are thus less suitable to indicate magnetic interactions.

As for nickelocenes and vanadocenes, $(Me_3SiCp)_2Ni$ and $(Me_3SiCp)_2V$ do follow the Curie law rather closely[23]. It was therefore of interest to find out why distinct deviations were found for **3NiNi**, **4NiNi**, **3VV**, and **5CrCr**.

The antiferromagnetic coupling derived from the $\chi_m T$-T curves (Table 3) is much too small to account for the ϑ-T curves of **3NiNi** and **3VV** in Figure 3. Interaction parameters $|J| < 15\ cm^{-1}$ should be clearly visible only below 200 K, a range which is hardly accessible by solution NMR spectroscopy. Furthermore, all reduced signal shifts $\vartheta(^1H)$ of **3NiNi** should increase with the temperature rather than decrease as found for the signals of Cp, 2-H, and 1,3-H. We also note that the signal of CH_3 shows the opposite trend whereas all trends are inverted for **4NiNi**.

The origin of these trends can be traced to the same phenomenon that has been discussed for the trends of the redox potentials and the NMR signal splittings, i.e. the folding of the bridging ligand of **3MM** and **5CrCr**. In the solid state **3CrCr** is folded as visualized in Figure 6A[7]. In solution the driving force for a folding should be the interaction between the terminal Cp ligands and the methyl groups of the bridge. The number of NMR signals of **3MM** is in accord with the folding shown in Figure 6B while **4MM** is expected to adopt the structure shown in Figure 6C. Intuitively, one predicts **4MM** to be more seriously distorted than **3MM**, and this is in accord with the NMR

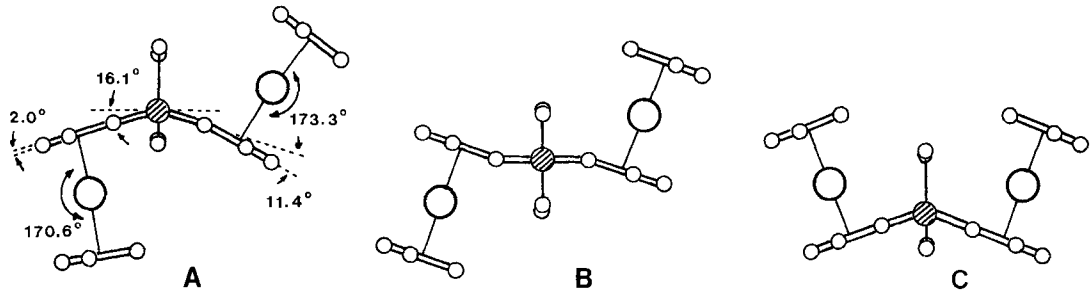

Figure 6. Folding of **3MM**; A: **3CrCr** in the solid state[7]; B and C: suggested folding of **3MM** and **4MM** in solution; the shaded atom is silicon

signal splitting discussed above. It must be also expected that the equilibrium structure changes with the temperature, which in turn, must influence the metal–ligand bonding. In agreement with this model the signal shifts of the five-membered ring protons of **3NiNi**, **4NiNi**, and **3VV** deviate from the Curie law (Figure 3a and b). By contrast, a change in the folding with little or no effect on the metal–ligand bonding should only influence the signal shifts of the methyl groups by hyperconjugation, a behavior which is not observed experimentally. In the *cis* isomers (cf. Figure 6C) the two CH_3 groups are nonequivalent, and the one pointing to the metal is oriented more favorably relative to the spin-carrying orbital. This is the basis for assigning the more shifted signal to the CH_3 group adjacent to the metal.

It follows that the magnetic interaction within these bridged metallocenes can be established safely only by magnetic measurements down to very low temperatures. The strength of the antiferromagnetic coupling given as J in Table 3 parallels the spin density found on the bridges. More examples are necessary, however, to demonstrate that simple NMR spectra may predict trends in magnetic interaction.

We gratefully acknowledge support from the *Deutsche Forschungsgemeinschaft*, the *Fonds der Chemischen Industrie*, the *Wacker Chemie GmbH*, the French-German exchange program *PROCOPE*, and the *Leonhard-Lorenz-Stiftung*. We also thank Dipl.-Chem. *H. Hilbig* for reproducing some NMR results.

Experimental

All manipulations were carried out with the exclusion of oxygen and moisture by using standard Schlenk equipment, NMR tubes with ground-glass joints and stoppers, and oxygen-free solvents. The glassware was flame-dried in vacuo. For some physical measurements sealed samples were used. Suspensions of **2** in THF were prepared as described in ref.[4]. – Medium-pressure liquid chromatography (MPLC) was performed with an apparatus from Kronwald (for details see ref.[10,11]). Cyclic voltammograms were recorded from solutions in purified propionitrile containing 0.1 M n-Bu_4NPF_6 as supporting electrolyte and with the equipment described earlier[10,11]. A Faraday balance[26] was used for the solid-state magnetic measurements. In the order **3NiNi**, **3CrCr**, and **3VV** the temperature range was 1.3–332.9 K, 1.3–293.9 K, and 1.3–295.5 K, the sample weight was 79.53, 12.482 and 6.788 mg, the diamagnetic correction was $-294 \cdot 10^{-6}$, $-304 \cdot 10^{-6}$, and -309.10^{-6} $cm^3\ g^{-1}$, respectively. The mass spectra were recorded with a Varian MAT 311A spectrometer (electron impact mode, 70 eV) and the NMR spectra with the spectrometers Bruker CXP 200, Bruker MSL 300, and Jeol JNM GX 270. The NMR signal shifts were measured relative to the solvent signals with signal shift values given in ref.[27] and referenced relative to the individual singal shift values of the corresponding diamagnetic dinuclear ferrocenes[11]. If not stated otherwise the spectra were taken at 305 K. The shifts were calculated to the standard temperature 298 K by assuming that the deviation from the Curie law is small in the narrow temperature range. The elemental analyses were carried out in the microanalytical laboratory of the Garching institute.

cis- and trans-Bis[(cyclopentadienyl)nickel]-μ-(1,2,3,3a,8a-η⁵:4a,5,6,7,7a-η⁵-3a,4,7a,8-tetrahydro-4,4,8,8-tetramethyl-4,8-disila-s-indacene-3a,7a-diyl) (**3NiNi**, **4NiNi**): Solutions of 8 mmol of **2** in 50 ml of THF and 80 mmol of CpNa in 150 ml of THF were combined and warmed to 50°C. When 15.7 g (48 mmol) of $NiBr_2(THF)_{1.5}$ was added in small portions with stirring the mixture became green. After stirring for another 2 h, THF was removed under reduced pressure, the remainder was extracted with hot hexane, and the solvent was removed again. From the dark green solid Cp_2Ni was separated by sublimation (10^{-2} Pa/60°C bath temperature), the remainder was dissolved in a minimum of hexane and the solution subjected to MPLC (column length/diameter 50/2.6 cm; silica gel Merck 60, 15–40 μm). Two small dark green bands developed first. The first one contained little residual Cp_2Ni and the second one a nickelocene with one Cp and monoprotonated **2** as ligands[28]. The main product was eluted as the third band. When the green solution was freed from the solvent and the resulting solid recrystallized from hexane at −30°C 2.98 g (76% based on **2**) of **3NiNi** was obtained as small green crystals. The mother liquor contained 0.2 g of a solid which was chromatographed again. Two overlapping bands were obtained: The first gave 0.15 g of **3NiNi**, thus increasing the yield to 80%; the second was a 9:1 mixture of **4NiNi/3NiNi** (^1H NMR, integration of the CH_3 signals). From a fourth yellow-green band 70 mg of a trinuclear NiNiNi derivative was obtained which will be reported on separately. – **3NiNi**: m.p. (rapid heating): 195–198°C (dec.); (slow heating): dec. at 180°C. – MS; *m/z* (%): 488 (100) [M^+], 473 (2) [$M^+ - CH_3$], 423 (13) [$M^+ - Cp$], 408 (2) [$M^+ - Cp - CH_3$], 300 (6) [$M^+ - CpNi - Cp$], 244 (16) [M^{2+}], 123 (7) [$CpNi^+$]; isotope pattern of M^+, *m/z* (% calcd./found): 488 (100/100), 489 (37.1/37.0), 490 (90.3/88.5), 491 (35.1/33.2), 492 (37.5/36.2), 493 (13.5/13.0), 494 (11.6/10.9), 495 (3.7/3.2), 496 (2.6/2.3). – $C_{24}H_{28}Ni_2Si_2$ (490.1): calcd. C 58.82, H 5.76, Ni 23.96, Si 11.46; found C 59.19, H 5.86, Ni 23.67, Si 11.90.

cis- and trans-Bis[(cyclopentadienyl)cobalt]-μ-(1,2,3,3a,8a-η⁵:4a,5,6,7,7a-η⁵-3a,4,7a,8-tetrahydro-4,4,8,8-tetramethyl-4,8-disila-s-indacene-3a,7a-diyl) (**3CoCo**, **4CoCo**): A solution containing 9 mmol of **2** and 90 mmol of CpNa in 150 ml of THF was

added with stirring to a mixture of 7 g (54 mmol) of $CoCl_2$, 100 ml of NEt_3, and 300 ml of THF. The dark brown suspension was stirred for 2 h and worked up as described for **3NiNi** to give 4 g of a crude product after subliming off Cp_2Co. The remaining solid was crystallized from hexane to give a mixture of cobaltocenes which were separated partly by fractional crystallization from hexane. The first fraction contained 0.9 g (20% based on **2**) of **3CoCo** as black microcrystals (m.p. 153°C). Later fractions contained **3CoCo** and increasing amounts of **4CoCo** up to a 3:2 mixture of **3CoCo/4CoCo** (^{1}H NMR). – **3CoCo**: $C_{24}H_{28}Co_2Si_2$ (490.5): calcd. C 58.77, H 5.75, Co 24.03, Si 11.45; found C 58.52, H 5.97, Co 23.20, Si 11.43.

trans-Bis[(cyclopentadienyl)chromium]-μ-(1,2,3,3a,8a-η⁵:4a,5,6,7,7a-η⁵-3a,4,7a,8-tetrahydro-4,4,8,8-tetramethyl-4,8-disila-s-indacene-3a,7a-diyl) (**3CrCr**): A mixture of 8.8 mmol of **2** and 70.3 mmol of CpNa in 120 ml of THF was treated with 9.0 g (46.3 mmol) of $CrCl_2$(THF) and worked up similarly as described for **3NiNi** except that MPLC was not applied. Instead, the hexane extract was freed from some insoluble material by filtering through Na_2SO_4. Rapid cooling of a solution which was saturated at 60°C to −20°C gave 1.81 g (43% based on **2**) of dark red-brown needles which decomposed at 155°C without melting. – MS; *m/z* (%): 476 (100) [M^+], 410 (9) [M^+ − Cp], 238 (14) [M^{2+}], 278 (16), 117 (12) [$CpCr^+$], 52 (15) [Cr^+]; isotope pattern of M^+, *m/z* (% calcd./found): 474 (9.7/10.9), 475 (4.8/6.1), 476 (100/100), 477 (59.3/59.7), 478 (28.0/28.1), 479 (8.7/8.7), 480 (2.1/5.3). – $C_{24}H_{28}Cr_2Si_2$ (476.7): calcd. C 60.48, H 5.92; found C 59.49, H 6.21.

trans-Bis[(cyclopentadienyl)vanadium]-μ-(1,2,3,3a,8a-η⁵:4a,5,6,7,7a-η⁵-3a,4,7a,8-tetrahydro-4,4,8,8-tetramethyl-4,8-disila-s-indacene-3a,7a-diyl) (**3VV**): 9.8 ml (67 mmol) of PEt_3 was added to a suspension of 12.5 g (33 mmol) of $VCl_3(THF)_3$ in 250 ml of THF. After stirring for 2 h, the purple solution was cooled to −78°C, and 22.5 ml of a 1.49 M solution of CpNa (33.5 mmol) was added dropwise within 30 min. The reaction mixture was warmed slowly to 50°C and stirred for 2 h. When the resulting blue solution was treated with 1.09 g (17 mmol) of zinc powder and heated to reflux for 5 h the color changed to purple. After cooling of the solution to −78°C, a suspension of 17 mmol of **2** in 100 ml of THF and 20 ml of TMEDA was added dropwise with stirring within 3 h. Then the mixture was allowed to warm to ambient temperature and stirred for another 12 h. The solvents were removed, the resulting solid was extracted with 300 ml of hot hexane and the extract reduced to a solution which was saturated at 55°C. Cooling to −40°C gave a crystalline material which was separated from the red-brown solution and washed with 10 ml of pentane. Recrystallization from THF (−40°C) gave 2.05 g (26% based on **2**) of **3VV** as black-violet crystals, m.p. 180−182°C (dec.). – MS; *m/z* (%): 474 (100) [M^+], 459 (3) [$M^+ - CH_3$], 358 (21) [M^+ − CpV], 343 (3) [$M^+ - CpV - CH_3$], 293 (25) [$M^+ - CpV - Cp$], 116 (20) [CpV^+]; isotope pattern of M^+, *m/z* (% calcd./found): 473 (0.5/1.7), 474 (100/100), 475 (37.1/36.7), 476 (13.0/13.8), 447 (2.7/3.2). – $C_{24}H_{28}Si_2V_2$ (474.5): calcd. C 60.75, H 5.95, Si 11.84, V 21.47; found C 60.51, H 6.01, Si 11.90, V 21.2.

trans-Bis[dichloro(triethylphosphane)chromium]-μ-(1,2,3,3a,8a-η⁵:4a,5,6,7a-η⁵-3a,4,7a,8-tetrahydro-4,4,8,8-tetramethyl-4,8-disila-s-indacene-3a,7a-diyl) (**5CrCr**): To a suspension of 7.6 mmol of **2** in 50 ml of THF which was cooled to −90°C was added 5.7 g (15.2 mmol) of $CrCl_3(THF)_3$. The violet mixture was allowed to warm to room temperature with stirring whereupon the color changed to dark blue. After replacement of THF by 100 ml of hexane, the mixture was treated with 2.3 ml (15.2 mmol) of PEt_3. Then the solvent was stripped, the solid residue extracted with $CHCl_3$, and the solution reduced. Upon cooling to −30°C 4.53 g (82% based on **2**) of **5CrCr** was obtained as dark blue cubes, m.p. 248°C (dec.). – $C_{26}H_{48}Cl_4Cr_2P_2Si_2$ (724.6): calcd. C 43.10, H 6.68, Cl 19.57, Cr 14.35; found C 42.94, H 6.46, Cl 19.35, Cr 14.50.

trans-[(Cyclopentadienyl)iron][(cyclopentadienyl)nickel]-μ-(1,2,3,3a,8a-η⁵:4a,5,6,7,7a-η⁵-3a,4,7a,8-tetrahydro-4,4,8,8-tetramethyl-4,8-disila-s-indacene-3a,7a-diyl) (**3FeNi**): A solution of 0.7 mmol of **6** in 60 ml of diethyl ether was prepared as described in ref.[10] and combined with a solution of 7 mmol of NaCp in 5 ml of THF. When 1.3 g (4 mmol) of $NiBr_2(THF)_{1.5}$ was added and the mixture was heated to reflux and stirred for 12 h a green solution resulted. Then the solvent was removed in vacuo, the solid residue was extracted with hot hexane, and the extract was freed from the solvent. Cp_2Ni was removed from the solid residue by sublimation (10^{-1} Pa/60°C bath temperature), and the remainder was worked up by MPLC as described for **3NiNi**. The following three bands were eluted: 1) A small green band containing little Cp_2Ni. 2) A light green band containing 0.24 g (71% based on **6**) of **3FeNi**. 3) A light green band containing a trinuclear FeNiFe species which will be reported on in a separate publication. The procedure gave similar yields when carried out in di-*n*-butyl ether (68%) and THF (64%). Occasionally, the precursor of **6**[10] was formed due to traces of water. In MPLC it appeared as an orange band soon after the band of Cp_2Ni. – **3FeNi**: Green microcrystals, m.p. 165°C. – MS; *m/z* (%): 486 (100) [M^+], 471 (6) [$M^+ - CH_3$], 421 (5) [M^+ − Cp] 243 (12) [M^{2+}], 123 (4) [$CpNi^+$]; isotope pattern of M^+, *m/z* (% calcd./found): 484 (5.6/8.0), 485 (2.1/3.8), 486 (100/100), 487 (39.5/39.1), 488 (51.9/52.0), 489 (19.7/19.3), 490 (11.9/12.0), 491 (5.5/3.6), 492 (2.4/2.2). – $C_{24}H_{28}FeNiSi_2$ (487.2): calcd. C 59.17, H 5.79, Fe 11.46, Ni 12.05, Si 11.53; found C 59.32, H 5.97, Fe 11.67, Ni 12.19, Si 10.90.

[1] [1a] P. Delhaas, M. Drillon (Eds.), *Organic and Inorganic Low Dimensional Crystalline Materials*, Plenum Press, New York and London, **1987**. – [1b] J. L. Brédas, R. R. Chance (Eds.), *Conjugated Polymeric Materials: Opportunities in Electronics, Optoelectronics, and Molecular Electronics*, Kluwer Akademic Publishers, Dordrecht, Boston, London, **1990**. – [1c] R. M. Laine (Ed.), *Inorganic and Organic Polymers with Special Properties*, Kluwer Academic Publishers, Dordrecht, Boston, London, **1992**.

[2] W. E. Geiger, N. G. Connelly, *Adv. Organomet. Chem.* **1985**, *24*, 87.

[3] O. Kahn, *Angew. Chem.* **1985**, *97*, 837; *Angew. Chem. Int. Ed. Engl.* **1985**, *24*, 834.

[4] J. Hiermeier, F. H. Köhler, G. Müller, *Organometallics* **1991**, *10*, 1787.

[5] [5a] U. Siemeling, R. Krallmann, P. Jutzi, *Abstr. IXth Int. Conf. Silicon Chem.*, Edinburgh, **1990**. – [5b] U. Siemeling, P. Jutzi, *Chem. Ber.* **1992**, *125*, 31. – [5c] U. Siemeling, P. Jutzi, B. Neumann, H.-G. Stammler, M. B. Hursthouse, *Organometallics* **1992**, *11*, 1328. – [5d] W. Mengele, J. Diebold, C. Troll, W. Röll, H.-H. Brintzinger, *Organometallics* **1993**, *12*, 1931.

[6] I. E. Nifant'ev, V. L. Yarnykh, M. V. Borzov, B. A. Mazurchik, V. I. Mstyslawsky, V. A. Roznyatovsky, Yu. A. Ustynyuk, *Organometallics* **1992**, *11*, 3739.

[7] H. Atzkern, J. Hiermeier, B. Kanellakopulos, F. H. Köhler, G. Müller, O. Steigelmann, *J. Chem. Soc., Chem. Commun.* **1991**, 997.

[8] R. M. Kowaleski, F. Basolo, W. C. Trogler, R. W. Gedridge, T. D. Newbound, R. D. Ernst, *J. Am. Chem. Soc.* **1987**, *109*, 4860.

[9] [9a] F. H. Köhler, R. Cao, K. Ackermann, J. Sedlmair, *Z. Naturforsch., B: Anorg. Chem., Org. Chem.* **1983**, *38*, 1406. – [9b] A. Grohmann, F. H. Köhler, G. Müller, H. Zeh, *Chem. Ber.* **1989**, *122*, 897. – [9c] D. S. Richeson, J. F. Mitchell, K. H. Theopold, *Organometallics* **1989**, *8*, 2570.

[10] M. Fritz, J. Hiermeier, N. Hertkorn, F. H. Köhler, G. Müller, G. Reber, O. Steigelmann, *Chem. Ber.* **1991**, *124*, 1531.

[11] H. Atzkern, J. Hiermeier, F. H. Köhler, A. Steck, *J. Organomet. Chem.* **1991**, *408*, 281.

[12] [12a] H.-M. Koepp, H. Wendt, H. Strehlow, *Z. Electrochem.* **1960**, *64*, 483. – [12b] T. Kakutani, Y. Morihiro, M. Senda, R. Takahashi, K. Matsumoto, *Bull. Chem. Soc. Jpn.* **1978**, *51*, 2847.

[13] D. Obendorf, H. Schottenberger, C. Rieker, *Organometallics* **1991**, *10*, 1293.

[14] [14a] J. D. L. Holloway, W. E. Geiger, Jr., *J. Am. Chem. Soc.* **1979**, *101*, 2038. – [14b] D. V. Kukharenko, E. M. Koldasheva, V. V. Strelets, *Dokl. Chem. (Engl. Transl.)* **1988**, *303*, 317.

[15] W. E. Geiger, Jr., *J. Am. Chem. Soc.* **1974**, *96*, 2632.

[16] [16a] F. H. Köhler, W. A. Geike, *J. Organomet. Chem.* **1987**, *328*, 35. – [16b] J. Blümel, N. Hebendanz, P. Hudeczek, F. H. Köhler, W. Strauss, *J. Am. Chem. Soc.* **1992**, *114*, 4223 and literature cited therein.

[17] A. Haaland, *Acc. Chem. Res.* **1979**, *12*, 415.

[18] P. Baltzer, A. Furrer, J. Hullinger, A. Stebler, *Inorg. Chem.* **1988**, *27*, 1543 and references cited therein.

[19] R. Prins, P. Biloen, J. D. W. van Voorst, *J. Chem. Phys.* **1967**, *46*, 1216.

[20] E. König, R. Schnakig, S. Kremer, B. Kanellakopulos, R. Klenze, *Chem. Phys.* **1978**, *27*, 331.

[21] [21a] F. H. Köhler, W. Prössdorf, *J. Am. Chem. Soc.* **1978**, *100*, 5970. – [21b] M. F. Rettig, R. S. Drago, *J. Am. Chem. Soc.* **1969**, *91*, 1361.

[22] J. Blümel, P. Hofmann, F. H. Köhler, *J. Magn. Reson.* **1993**, *31*, 2.

[23] F. H. Köhler, W. A. Geike, *J. Magn. Reson.* **1983**, *53*, 297.

[24] [24a] F. H. Köhler, K. H. Doll, W. Prößdorf, J. Müller, *Angew. Chem.* **1982**, *94*, 154; *Angew. Chem. Int. Ed. Engl.* **1982**, *21*, 151; *Angew. Chem. Suppl.* **1982**, 283. – [24b] D. A. Lemenovski, I. F. Urazowski, Yu. K. Grishin, V. A. Roznyatovsky, *J. Organomet. Chem.* **1985**, *290*, 301. – [24c] J. Heck, G. Rist, *J. Organomet. Chem.* **1988**, *342*, 45. – [24d] F. H. Köhler, J. Lachmann, G. Müller, H. Zeh, H. Brunner, J. Pfauntsch, J. Wachter, *J. Organomet. Chem.* **1989**, *365*, C15. – [24e] B. Bachmann, F. Hahn, J. Heck, M. Wünsch, *Organometallics* **1989**, *8*, 2523. – [24f] F. Bottomley, D. E. Paez, L. Sutin, P. S. White, F. H. Köhler, R. C. Thompson, N. P. C. Westwood, *Organometallics* **1990**, *9*, 2443. – [24g] R. Poli, H. D. Mui, *Inorg. Chem.* **1991**, *30*, 65.

[25] [25a] F. H. Köhler, R. Cao, G. Manlik, *Inorg. Chim. Acta* **1984**, *91*, L1. – [25b] H. Eicher, F. H. Köhler, *Chem. Phys.* **1988**, *128*, 297.

[26] F. H. Köhler, N. Hebendanz, G. Müller, U. Thewalt, B. Kanellakopulos, R. Klenze, *Organometallics* **1987**, *6*, 115.

[27] H. O. Kalinowski, S. Berger, S. Braun, *^{13}C-NMR-Spektroskopie*, Georg Thieme Verlag, Stuttgart, New York, **1984**, p. 74.

[28] P. Bergerat, J. Blümel, M. Fritz, J. Hiermeier, P. Hudeczek, O. Kahn, F. H. Köhler, *Angew. Chem.* **1992**, *104*, 1285; *Angew. Chem. Int. Ed. Engl.* **1992**, *31*, 1258.

[226/93]